Investigation of reaction mechanism and kinetic modelling for the toluene total oxidation in presence of CoAlCe catalyst

Eric Genty, Stéphane Siffert, Renaud Cousin

Investigation of reaction mechanism and kinetic modelling for the toluene total oxidation in presence of CoAlCe catalyst

E.Genty [1, $, *], S.Siffert[1], R.Cousin [1*]

[1] Unité de Chimie Environnementale et Interactions sur le Vivant (UCEIV), Université du Littoral Côte d'opale, Dunkerque, 59140, France

Corresponding author: E-mail: eric.genty@univ-lille1.fr, Renaud.Cousin@univ-littoral.fr

Abstract

Hydrotalcite like compounds containing Co, Al and Ce are synthesized by co-precipitation method. The mixed oxides issued from calcination step, have been characterized and tested for the toluene total oxidation with various concentration of toluene and oxygen. The toluene conversion curves have been modelled in this paper with eight models. The Mars Van Krevelen mechanism shows the bestr accordance with the experimental data. Moreover, the determination of the Co_3O_4-CeO_2 interface as the active center have been performed with the experimental observations. The Co_3O_4 allows obtaining high catalytic activity, and the CeO_2 permits increasing the reoxidation of the Co_3O_4 to perfume a new catalytic cycle.

Keywords: Mixed oxide, Ceria, Cobalt oxide, Toluene oxidation, kinetics modelling, Catalytic oxidation

1. Introduction

In recent years, environmental legislation has imposed increasing stringent targets for permitted levels of atmospheric emission. Volatile Organic Compounds (VOCs) as one of the main atmospheric pollutants are evacuated to the atmosphere from a wide variety of gaseous emissions, such as automobile exhaust petrochemical processes, treatment of the solid and liquid wastes. These regulations have induced the development of different methods for the elimination of VOC [1–3]. These methods can be classified in two groups: non-destructive and destructive. In the non-destructive methods, VOC are retained, without chemical transformation. Adsorption, absorption and condensation are included in this group. The destructive methods transform VOC into other compounds, inert or less dangerous. Thermal incineration and catalytic oxidation are included in this second group. Catalytic total oxidation is a technique in which pollutants, usually contained in a gaseous stream, are oxidized completely (into carbon dioxide and water molecules) in the presence of a catalyst. It has the advantages of providing nearly total elimination of pollutants, with lower generation of organic by-products at moderate temperatures (approximately 300 °C), hence with low operation cost. VOC destruction processes are applied often for low pollutant concentration. In this case, working at low temperature is important. For this reason an active catalyst able to transform VOC into carbon dioxide and water is required [1].

Two types of catalysts for the catalytic treatments of VOC are used in these processes: transition metals based oxides (Co, Cu, Mn,...) and noble metals supported (Pt, Pd, Rh, ...) [4–7]. It is generally accepted that noble metal-based catalysts are preferred when aromatic compounds are involved in the reaction due to the low temperature for the total conversion. However, due to the high cost of the

noble metals, many researchers devoted to the development of suitable catalysts containing only transition metal oxides [8–13]. Hydrotalcite-like compounds (HTlc) are presented as precursors of mixed oxides, with an enormous potential for the generation of well dispersed, active and very stable catalysts for several applications. This class of layered double hydroxides consists of positively charge metal hydroxide layers separated from each other by anions and water molecules. A wide range of possible cations and anions that could be incorporated in the Hydrotalcite (HT) structure gives rise to several different materials [14–16]. Indeed after oxidation treatment, mixed oxides are formed and possess unique properties like high surface area and porosity, good thermal stability, good mixed oxides homogeneity and undergo well metal cation dispersion [17,18].

The interest in the application of calcined hydrotalcite like compounds (mixed oxides) as catalyst in the environmental field is very important. For example, the mixed oxides are very active and selective in the decomposition of nitrogen oxides [19] or in the total oxidation of Volatile Organic Compounds [11, 16]. The mixed oxides obtained after calcination are used equally as catalysts [15,20,21] or as catalytic support [19,20,22] in redox reactions such as the selective oxidation of hydrocarbons, in the total oxidation reaction of volatile organic compounds and carbon monoxide oxidation [15,16,21,23]. The mixed oxides containing cobalt and aluminum issued from the hydrotalcite precursor show a good catalytic activity for the VOC total oxidation [21,23,24]. The key determining factors in the activity of the cobalt oxides solids are the nature and distribution of these species on the solid surface for the supported catalysts [25,26]. The preparation methods, the nature of the support and the precursors, the metal loading have an influence on the cobalt

oxides species state [27–29]. The use of metallic oxides with promoters can lead to an improvement in the oxygen storage capacity, which evidently enhances the oxidation processes [10,11]

In previous work [30], we have studied the influence of Ce in the hydrotalcite structure. Adding Ce in the solid allows to obtain, after calcination, an efficient catalyst for the toluene total oxidation which possess higher reducibility properties. Their catalytic activity has been correlated to the reducibility properties. Thus, for this study, a catalyst presented the best activity in toluene total oxidation has been chosen for this kinetic investigations. This catalyst developed in our laboratory was denominated as $Co_6Al_{1.2}Ce_{0.8}HT500$

In this present paper, we have performed a kinetic study of the toluene total oxidation reaction. The aim of this work is the modelling of the chemical reaction by eight models for the toluene total oxidation in presence of this CoAlCe mixed oxide. The catalytic test will be completed by physico-chemical characterizations.

2. Experimental

2.1. Preparation of Catalysts

For the synthesis of the mixed oxides by hydrotalcite way, the co-precipitation method is used [30,31]. An aqueous solution of 200 mL was prepared with appropriate amounts of $Co(NO_3)_2,6H_2O$, $Al(NO_3)_3,9H_2O$ and $(Ce(NO_3)_3,6H_2O)$ with a molar ratio of Co^{2+}/M^{3+} of 6/2 (solution A). This solution was added dropwise to 300 mL of a Na_2CO_3 solution (1 $mol.L^{-1}$, solution B). The pH of the additive solution was maintained at 10.5 with a NaOH solution (2 $mol.L^{-1}$). After addition, the suspension was stirred for 24 hours at room temperature. Then, the latter was filtered and

washed with hot deionized water (~ 60 °C). The solid obtained was dried in an oven for 64h at 60°C before grinding. The hydrotalcite intermediate was denominated $Co_6Al_{1.2}Ce_{0.8}HT$

A thermal treatment was performed under flow of air (4 $L.h^{-1}$, 1 $°C.min^{-1}$, 4 hours at 500 °C) to obtain a mixed oxide. The calcined material was designated by $Co_6Al_{1.2}Ce_{0.8}HT500$. [31].

2.2. Characterization Techniques.

Crystallinity of solids is determined by X-Ray Diffraction (XRD) technique with a Bruker D8 Advance diffractometer equipped with a copper anode (λ = 1.5406 Å) and a LynxEye Detector. The scattering intensities are measured over an angular range of 10° ≤ 2θ ≤ 80° for all samples with a step-size of Δ(2θ) =0.02° and a count time of 4s per step. The diffraction patterns have been indexed by comparison with the “Joint Committee on Powder Diffraction Standards” (JCPDS) files.

The specific surface areas of solids were determined by the BET method using a QSurf M1 apparatus (Thermoelectron), and the N_2 adsorption at -196°C.

Elemental compositions of samples were analysed using an iCAP-6300-DUO ICP-OES (Thermo Electron). 50.0 mg of powder were dissolved in 5 mL of aqua regal (HNO3/HCl 1:2) under microwave during 30 min (model MARSXpress, CEM). The solution was diluted extended to 50.0 mL with ultrapure water, and then diluted at 10 % and filtered with a 0.45 µm cellulosic micro-filter

2.3. Catalytic tests

The activity for toluene total oxidation of the catalysts (100 mg) was measured under continuous flow system in a fixed bed reactor at atmospheric pressure. Before each

test, the catalyst was reactivated in flowing air (2L.h^{-1}) at 500°C for 4 hours. The flow of the reactant gases (100 mL.min^{-1} with 1000 ppm of C_7H_8 and 20%O_2 in He) was adjusted by a Michell apparatus constituted of a saturator, and mass flow controllers. The space velocity was calculated and equal to 30 L.h^{-1}.g^{-1} for all catalytic test. Moreover, in the kinetic analysis, the concentration of toluene was composed between 500 and 2000 ppm while the concentration of oxygen was between 0.3 and 20%. After reaching a stable flow, reactants passed through the catalyst bed and the temperature was increased from room temperature to 400°C (1°C.min^{-1}). The feed and the reactor outflow gases were analysed on line by a micro-gas chromatograph (Agilent 490 Micro gas chromatography) and infrared analysers (ADEV 4400 IR). The catalysts performance was assessed in terms of T_{50} temperature, which corresponds to the temperature of 50% conversion.

The toluene conversion was calculated considering products and by-products and in function of carbon number for each compound:

$$X_T = \left(\frac{[CO_2]_T + [CO]_T + [C_6H_6]_T * 6}{[CO_2]_T + [CO]_T + [C_6H_6]_T * 6 + [C_7H_8]_T * 7} \right) * 100$$

Where:

- X_T is the toluene conversion at the *T* temperature (%);

- $[I]_T$ is the concentration of the compound *I* at the *T* temperature (ppm).

Following the using of a plug flow reactor, the toluene oxidation rate was determined by the following equation:

$$r = \frac{Q}{V_{mol}} \frac{273{,}15}{T_{exp}} \frac{[Tol]_0}{10^6} \frac{X_{tol}}{m_{cata}}$$

Where:

r = toluene oxidation rate ($mol.g^{-1}.h^{-1}$),

Q = flow rate ($L.h^{-1}$),

T_{exp} = Temperature of analysis (K),

V_{mol} = 22,4 $L.mol^{-1}$,

X_{tol} = VOC conversion (%),

m_{cata} = catalyst mass (g).

3. Results and discussion

3.1 Physicochemical characterizations of $Co_6Al_{1.2}Ce_{0.8}HT$ sample.

X-rays diffraction patterns of the dried and calcined samples are reported on the Figure 1.

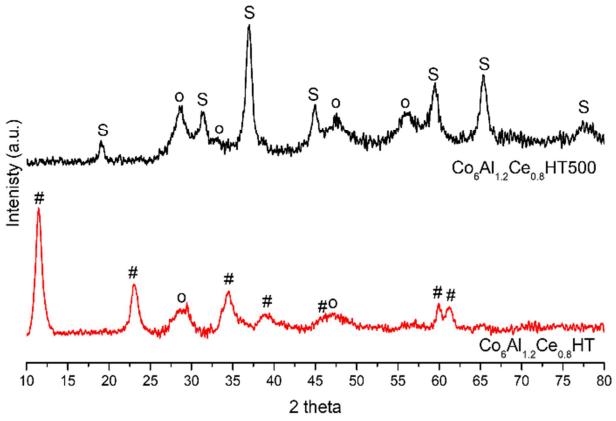

Figure 1 **XRD patterns for $Co_6Al_{1.2}Ce_{0.8}HT$ and $Co_6Al_{1.2}Ce_{0.8}HT500$ samples (#: $Co_6Al_2(OH)_{16}CO_3$, $4H_2O$, S: Co_3O_4, $CoAl_2O_4$ or Co_2AlO_4, o: CeO_2)**

The XRD pattern reveals the typical diffractograms of hydrotalcite like compounds. The cobalt-aluminium hydrotalcite phase (ICDD-JCPDS files 51- 0045 noted #) is observed for the dried sample. Moreover, a second phase corresponding to the CeO_2 phase is also observed (ICDD-JCPDS files 34-0394 noted o). This phase is explained by the partial substitution of Al^{3+} by Ce^{3+} in the hydrotalcite structure. Concerning the calcined samples, two crystalline phases are observed: the spinel phases of Co_3O_4 (JCPDS-ICDD file 42-1467) or $CoAl_2O_4$ (JCPDS-ICDD file 44-0160) or Co_2AlO_4 (JCPDS-ICDD file 38-0814) and the ceria phase CeO_2 (JCPDS-ICDD file 34-0394). The three spinel phases cannot be distinguished because their characteristic diffraction peaks are close in intensity and position. The metal ratio and the porosity characteristics are reported in table 1. The chemical ratio measured is in accordance with the theoritical composition.

Table 1 Physico-chemical characterizations of the $Co_6Al_{1.2}Ce_{0.8}$HT500 sample.

Sample	Specific surface area ($m^2.g^{-1}$)	Pore diameter ($cm3.g^{-1}$)	Co/Al/Ce molar ratio	
			Theorical	Experimental
$Co_6Al_{1.2}Ce_{0.8}$HT500	108	3.7	6/1.2/ 0.8	6/1.22/0.73

3.2 Total oxidation of Toluene

This part concerns the influence of toluene and oxygen concentration in the reactive flow. Firstly, a study concerning the toluene concentration have been performed. The concentration of toluene is composed between 500 and 2000 ppm of toluene with a flow equals to 100 mL/min and an oxygen concentration equals to 20%. The curves

representing the toluene conversion versus the temperature are reported on the Figure 2a.

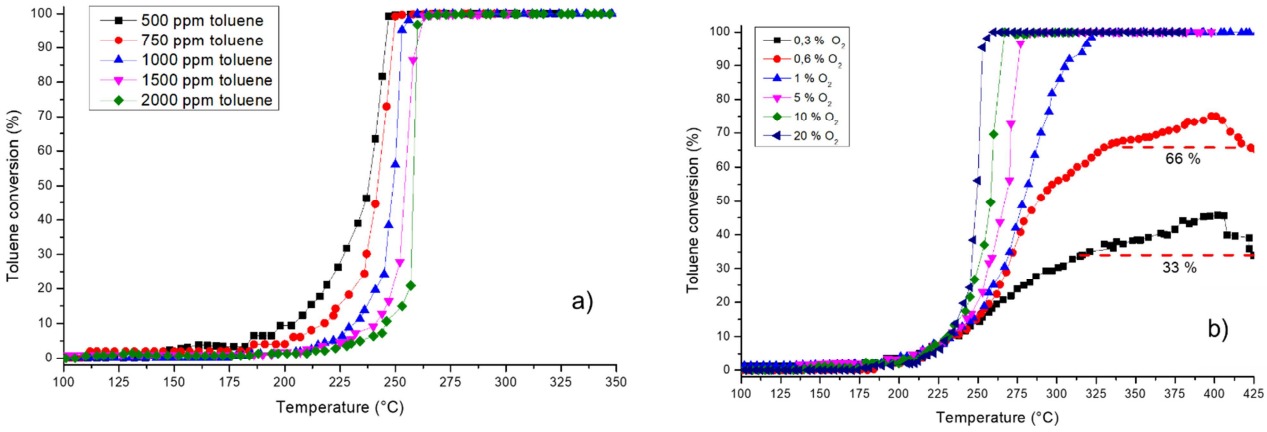

Figure 2: Toluene conversion curves with variation of toluene concentration (a) and oxygen concentration (b)

The catalytic performance of CoAlCe mixed oxide has been also compared to the literature and the T_{50} have been reported in Table 2.

Table 2 Results observed for catalytic toluene oxidation.

Sample	Toluene	Space Velocity ($L.h^{-1}.g^{-1}$)	T_{50} (°C)	Ref.
$Co_6Al_{1.2}Ce_{0.8}HT500$	1000 ppm	30	248	This work
0.5% Pd/γ-Al_2O_3	1000 ppm	30	197	[32]
Pt-Pd/Al_2O_3-CeO_2	1000 ppm	70	270	[33]
Pt-Pd/Al_2O_3	1000 ppm	70	214	[33]
0.5% Pd/MgAlHT	1000 ppm	30	216	[24]
0.5% Pd/TiO_2	1000 ppm	10	224	[34]
Co30Ce	1000 ppm	36	233	[13]

MnCuAl	800 ppm	75	258	[35]
Co_6Al_2HT	1000 ppm	30	287	[36]

The CoAlCe mixed oxide, shows interesting performance compared to the literature and especially compared to the other mixed oxide catalysts used in similar conditions. Firstly, we can notice that the catalytic reactivity depends to the toluene concentration. Indeed, the increase of the toluene partial pressure involves a shift to the higher temperature for toluene conversion. These measures could be indicate a partial order concerning the toluene lower than 1. This hypothesis will be tested when the power law modelling will be performed in the following section. Concerning the influence of oxygen concentration, this latter have been modified in the range between 0.3% (3000 ppm) and 20% and the toluene concentration has been fixed to 1000 ppm. The experiments in presence of 0.3 and 0.6% correspond to the under stoichiometric study for oxygen, following the chemical reaction ($C_7H_8 + 9\,O_2 \rightarrow 7\,CO_2 + 4\,H_2O$). The experiment with 1% of oxygen in the mixture corresponds to the stoichiometric study. The curves representing the toluene conversion in presence of the various oxygen contents are reported on the Figure 2.b.

Firstly, we can be observed that the decreasing of the partial pressure on oxygen induces an increasing of the temperature needed for the total conversion of toluene. However, before 240°C corresponding to the conversion lower than 20% for toluene, any modifications for the toluene conversion have been observed in function of oxygen proportion in the reactive flow. These measures could be indicated that the partial order concerning the oxygen is close to 0. This hypothesis will be evaluated in

the power law modelling in the following section. However, the main difference observed concerns the high conversion, Indeed, to complete the oxidation of toluene, higher temperature is needed for the low oxygen concentration. Moreover, for the 0.3 and 0.6% experimotents, toluene is not completely converted. This is due to the non-stoichiometric conditions. However, in presence of 0.3% of oxygen, 45% of toluene have been observed at 400°C, and decrease to the theoretical value (33%) at 450°C. A similar observation is performed for the catalytic test with 0.6% of oxygen, with an over conversion of toluene to obtain 75% at 400°C and decrease to the theoretical value (66%) at 450°C. These over conversions of toluene higher than the theoretical conversion, will be explained by the consumption of oxygen present in the catalyst. This observation will be in accordance by the Mars Van Krevelen mechanism (redox mechanism).

To understand, this over-conversion of toluene, XRD analysis after catalytic test with lower oxygen concentration have been performed (0.3 and 20% of oxygen). Thus, on these XRD analyses, it could be observed modification of the oxide phase during the catalytic test. The diffractograms of the both samples are reported on the Figure 3.

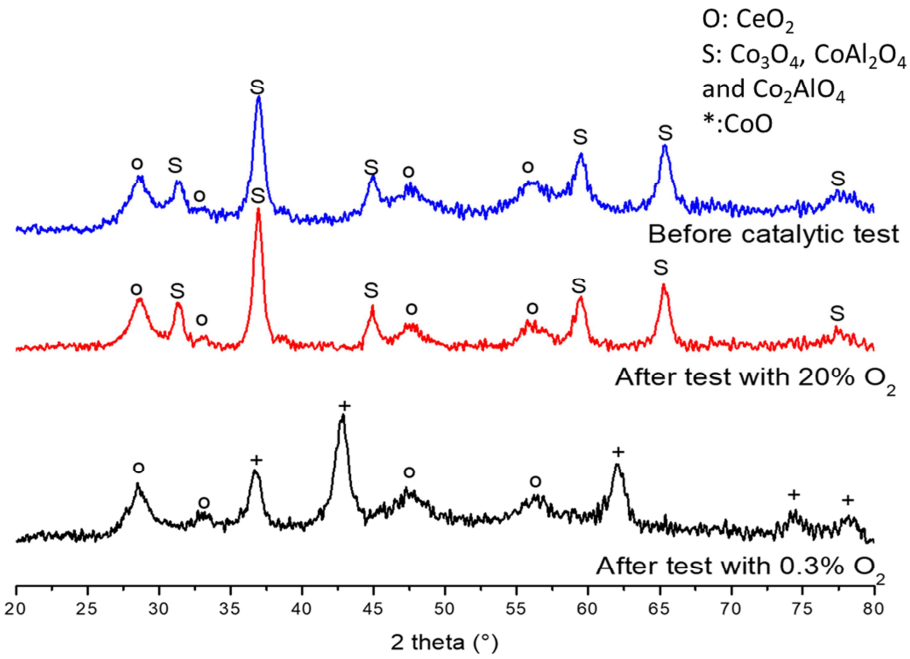

Figure 3 : XRD patterns for CoAlCe before, after test with 20% of O_2 and after test with 0.3% of O_2

Concerning the solid issued from the 20% of oxygen catalytic test, 2 crystalline phases are observed: the spinel phases of Co_3O_4 (JCPDS-ICDD file 42-1467) or $CoAl_2O_4$ (JCPDS-ICDD file 44-0160) or Co_2AlO_4 (JCPDS-ICDD file 38-0814) and the ceria phase CeO_2 (JCPDS-ICDD file 34-0394). These phases are already present in the catalyst before the catalytic test. Concerning the solid issued from the 0.3 % oxygen test, the ceria phase is also present while the spinel phases of cobalt or cobalt aluminium are not revealed. Indeed, the cobalt is present in the sample only in cobalt oxide form CoO JCPDS-ICDD file 72-1474). The observation of only cobalt oxide phase suggests that the CoAl spinel phases are in minority compared to the Co_3O_4. The presence of cobalt only in Co^{2+} species indicates a partial reduction of this species during the catalytic test. This partial reduction of the cobalt species is explained by the using of oxygen of Co_3O_4 species during the toluene oxidation. The presence of ceria after test could be explained by the fact that is not the active phase

of the solid but allows re-oxidising the cobalt oxide after the liberation of their oxygen. Moreover, the over – conversions with the low oxygen quantity, need to consume $3.0\ 10^4$ ppm of oxygen atoms. This oxygen quantity is calculated considering the over-conversion of toluene and the atomic oxygen needed for the chemical reaction of toluene oxidation. If we consider the partial reduction of Co_3O_4 into CoO during the catalytic reaction, we observe a quantity of atomic oxygen equal to $3.1\ 10^3$ ppm. This quantity of atomic oxygen is lower than the total oxygen needed to perform this over conversion that could be confirm that the hypothesis than the catalytic oxidation takes place on the Co_3O_4 species and confirm the possible Mars Van Krevelen mechanism. With these different hypotheses, a reaction scheme could be do for the $Co_6Al_{1.2}Ce_{0.8}$HT500 (Figure 4).

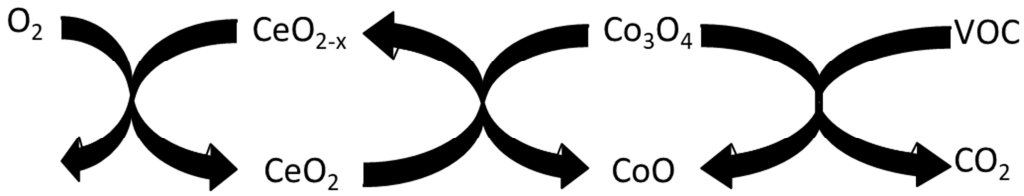

Figure 4 : Reaction mechanism for the toluene total oxidation with $Co_6Al_{1.2}Ce_{0.8}$HT500 catalyst.

This scheme takes into account the oxidation of the toluene (named VOC) into carbon dioxide by the reduction of Co_3O_4 into CoO. After that, the CoO is reoxidised by the use of Ce^{3+}/Ce^{4+} and the high mobility of the oxygen in the mixed oxide matrix. After observed the behaviour of the catalytic material with various toluene and oxygen concentrations in the reactional mixture, different kinetic models have been studied and discussed to explain the observation performed previously.

3.3. Modelling with the power law

The first model tested in this paper corresponds to the power law. This model purely mathematical is generally used in the literature like the first approach to obtain kinetic information [16,37–39]. This model express the toluene oxidation rate in function of toluene and oxygen partial pressures (P_{tol} and P_{O2}), both assigned a power coefficient corresponding to the partial order of the species (n and m). The kinetic expression of the power law is reported in Table 3.

The apparent rate constant (k) presents in the mathematic expression of the power law follows the Arrhenius law.

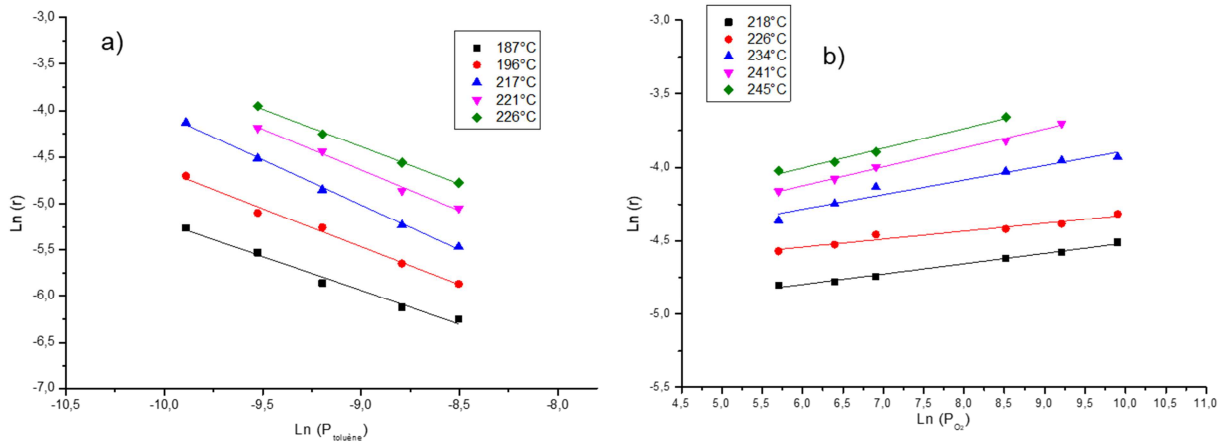

Figure 5: Determination of the partial order for toluene (a) and oxygen (b)

The Figure 4a, represents the logarithm of the reaction rate in function of the logarithm of toluene partial pressure for five selected temperatures (187, 196, 217, 221, 226 °C). These temperatures have been choose to obtain a toluene conversion lower than 20% for each case. The slope permits to determine apparent order for the toluene. The hypothesis suggested previously is confirmed with an apparent order concerning the toluene equal at -0.86. A similar study is performed for the oxygen

partial pressure (Figure 5b). For this study, five others temperatures have been choose (218, 226, 234, 241 and 245°C). At this temperature, the conversion of toluene and oxygen is lower than 20%. The slope in this case is equal to 0.10. This order close to 0 is not surprising. Indeed, in the literature, to simplify the kinetic study, an apparent order equal to 0 is often choose. Krishnamoorthy et al. [40] have been observed that the oxygen concentration have an effect when it was inferior to 3% for the conversion of the 1,2-dichlorobenzen. When this concentration is higher than 3%, there is low influence on the catalytic activity. To determine the activation energy and the pre exponential factor, we can plot the neperian logarithm of the rate (ln(r)) versus the inverse of the temperature (1/T). The Figure 6 represents the Arrhenius plot for the conversion inferior to 20% in the case of the reactive flow is the following: 1000 ppm of toluene and 20% of dioxygen. This pre-exponential factor is in relationship with the number of active sites in the catalytic materials. The slope of this graphic is equal to Ea/RT and permits to determine the activation energy of the catalytic reaction.

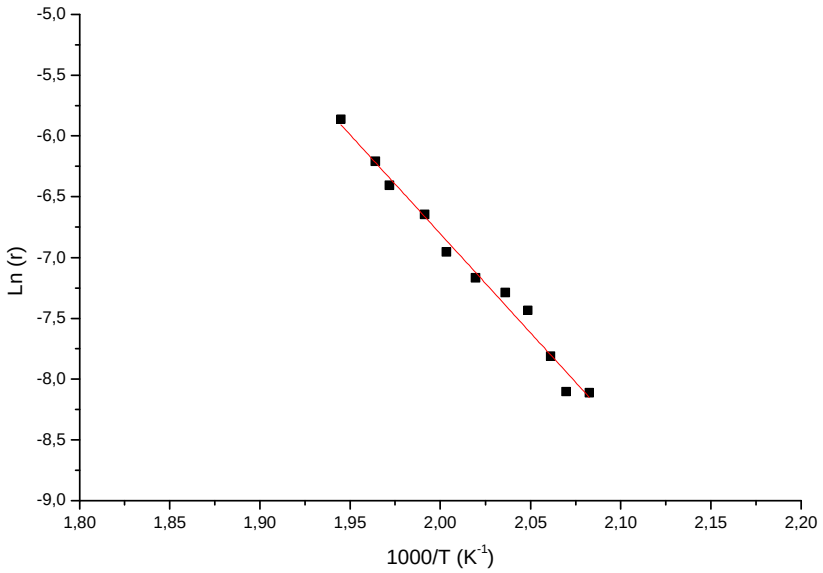

Figure 6: Determination of energy activation for the $Co_6Al_{1.2}Ce_{0.8}$HT500

A comparison of the activation energy obtained with the literature could be done. Choudary *et al.* [37] and Delimaris *et al.* [41] have been observed for the toluene total oxidation an activation energy between 80 and 110 kJ/mol for non-noble metal based catalysts. Moreover, Gennequin *et al.* [16] have been show that a CoAl mixed oxide issued from hydrotalcite precursor has a activation energy equal to 90 kJ/mol for similar conditions. This study shows equally a partial order for toluene equal to -1 and 0.2 for the oxygen. Using the parameters obtained during this study, a toluene conversion curve have been simulated and compared to the experimental curve (Figure 7).

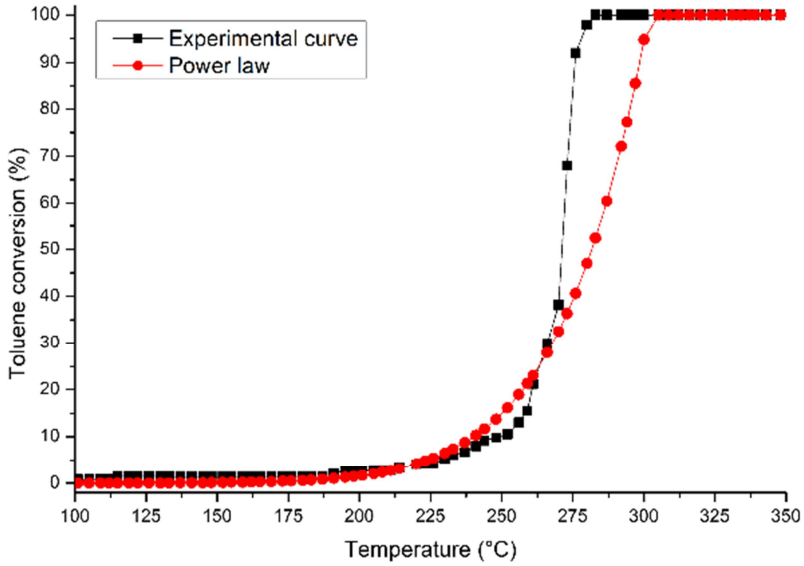

Figure 6 : Comparison of experimental curve : experimental and power law simulation

The simulation shows a good accordance with the experimental values at lower conversion. However, when the conversion is higher than 30%, a difference is observed. It could be explained by the exothermicity of the catalytic reaction. Moreover the model is particularly focused on the chemical regime when the conversion is lower than 20 %. The local temperature increase during the catalytic reaction and is not reported in the power law model. To conclude for this model, the observation of a negative partial order for the toluene indicates an inhibitor effect for the toluene due to the high adsorption of this one on the catalytic material's surface. In order to determine with more information the reaction mechanism, the Elay Rideal Model was tested.

3.4. Eley – Rideal model

The Eley-Rideal model is derived from the Langmuir Hinshelwood model [42]. In this latter named model, the catalytic reaction has been performed at the catalyst surface between two adsorbed species. In case of VOC total oxidation, this mechanism

implies the surface reaction between oxygen and VOC compound. The adsorption of VOC and O_2 could be dissociative or not and a competition is possible between these two species. This mechanism is often used for the VOC total oxidation in presence of noble metal based catalyst [43,44]. In case of Eley-Rideal mechanism, the catalytic reaction takes place at the catalytic surface between an adsorbed specie and a second in the gas phase. This mechanism is often reported and show interesting result concerning the total oxidation of VOC in presence of reducible catalytic support with noble metal [44,45]**.** In this paper, the both mechanisms have been considered and the Eley-Rideal model has been tested (for the toluene adsorbed and for the toluene in gas phase (oxygen adsorbed)). The kinetic expressions for the two Eley-Rideal models and Langmuir Hinshelwood model are reported in Table 3.

As in the case of Power Law model, the apparent rate constant (k_r) follows the Arrhenius law .The adsorption rate constant for oxygen and toluene follows the Van't Hoff relation. For the toluene, the relation is as following:

$$K_{tol} = K'_{tol} \exp\left(\frac{-\Delta H_{ads_{tol}}}{RT}\right)$$

with K_{tol} = adsorption rate constant for the toluene (Pa^{-1}), K'_{tol} = Pre exponential factor for toluene adsorption (Pa^{-1}), $\Delta H_{ads_{tol}}$ = Toluene adsorption enthalpy ($J.mol^{-1}$)

These models, more complex than the power law model, take into account the reaction rate and the adsorption enthalpy of toluene or oxygen. To determine all values, the apparent rate constant could be firstly determined. To define the values of the constants and the energy, the same experimental points than the power law have been taken into account. A similar methodology than for the power law modelling, has been used to determine the k_r and K_{tol} or K_{O2}.

The values of the different parameters are reported in Table 3. Concerning the adsorption enthalpy of toluene or oxygen, the negative value observed indicates that the adsorption of these species is exothermic. Moreover, it could be noticed that in comparison the two models, the pre exponential factor is higher in case of E-R2 than the E-R1 model. This change indicates that toluene possess a better affinity for the catalytic material than oxygen. Considering the value reported in Table 3, the conversion curves have been plotted (Figure 8) for the three new models and compared to the power law model and the experimental curve.

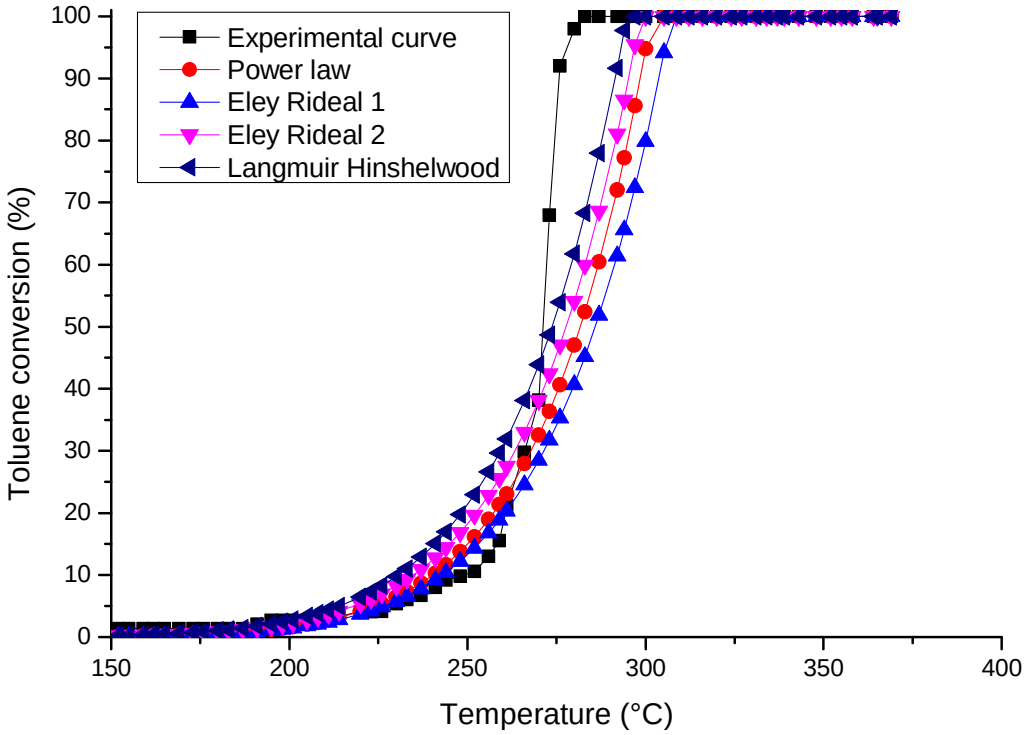

Figure 8 : Comparison of experimental curve : experimental, power law simulation, Eley Rideal (2 models) and Langmuir Hinshelwood

We can notice firstly, that the correlation between the experimental values and the Eley-Rideal model are not sufficient to explain the result obtained previously. The Langmuir Hinshelwood shows better correlation and is in accordance with the

literature observation which indicates that the L-H model is generally used for the modelling of the reactivity for the VOC total oxidation [38,46]. However, the difference between the experimental values and the L-H model is important and this model does not explain totally the reactivity of the solid. To continue this study, the Mars Van Krevelen mechanism has been studied.

3.5. Mars Van Krevelen model

The Mars Van Krevelen mechanism (MVK) often describes for the total oxidation of hydrocarbon on oxide metal catalyst. In this redox mechanism, the reactive species is an oxygen atom present in the bulk of the catalyst (O^{2-}), and reacts with the hydrocarbon. This oxygen atom is regenerated by the adsorption of oxygen of the gaseous phase during the second step. The main steps have been performed with a cyclic manner. Two steps could resume this mechanism:

The reduction of the oxide catalytic material (Cat-O) with the hydrocarbon (R):

$$Cat - O + R \xrightarrow{K_{tol}} Cat + R - O$$

The oxidation of the reduced catalytic material (Cat) by the adsorption of oxygen:

$$2Cat + O_2 \xrightarrow{K_{O2}} 2\,Cat - O$$

The determining rate is often the first step, corresponding to the reduction of the catalytic material. Thus, taking into an account the presence of a high reducible mixed oxide at low temperature it could explain the presence of high activity at low temperature in case of total oxidation of VOC. So, this mechanism is also reported than shows interesting results for the total oxidation of VOC in presence of reducible metal oxides [46–49]. The mathematical expression of Mars Van Krevelen (MVK)

mechanism is mentionned in the Table 3. The rate constant (K_{O_2}, K_{tol}) in the mathematic expression follow the Arrhenius law. The Figure 9 reports the plot for the determination of the activation energy corresponding to the rate constant.

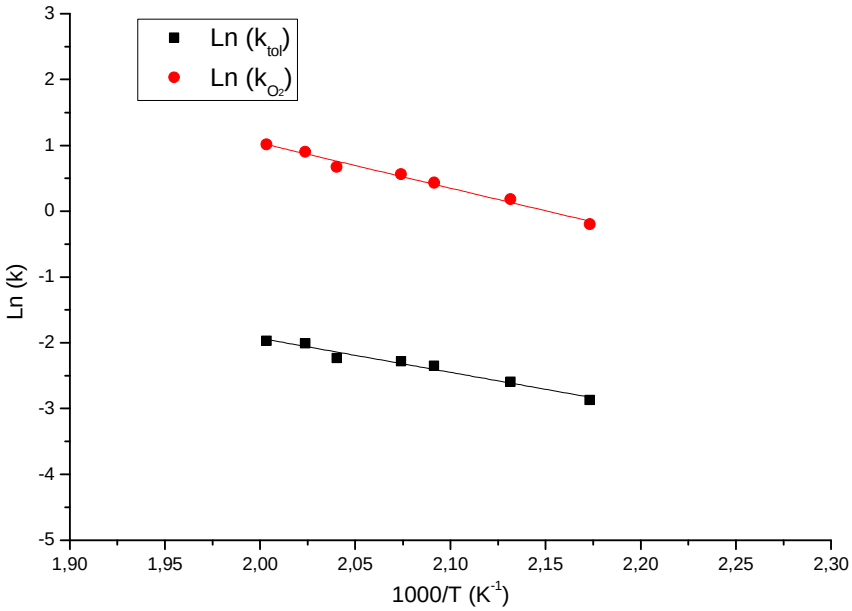

Figure 9: Determination of kinetic parameters for Mars Van Krevelen mechanism

The values of ~~the different~~ parameters are reported in Table 3. We can notice that the toluene oxidation rate constant is lower than the catalyst re-oxidation constant. This is in accordance with the Mars Van Krevelen model where the first step is the slower step. The values obtained for this model are quite similar than the values observed in the literature [50–52]. Indeed, Choudhary *et al.* [37] have observe similar results for the toluene oxidation. However, they revealed also an activation energy higher in case of the reoxidation of the catalytic material for the toluene oxidation with Fe/ZrO_2 material. Ordonez *et al.* [50] have also report an activation energy higher in case of toluene oxidation compared to the reoxidation catalyst for a Pt/Al_2O_3 catalyst.

The conversion curve of toluene modelled by MVK model is represented in Figure 9 and compared to others models and experimental curve.

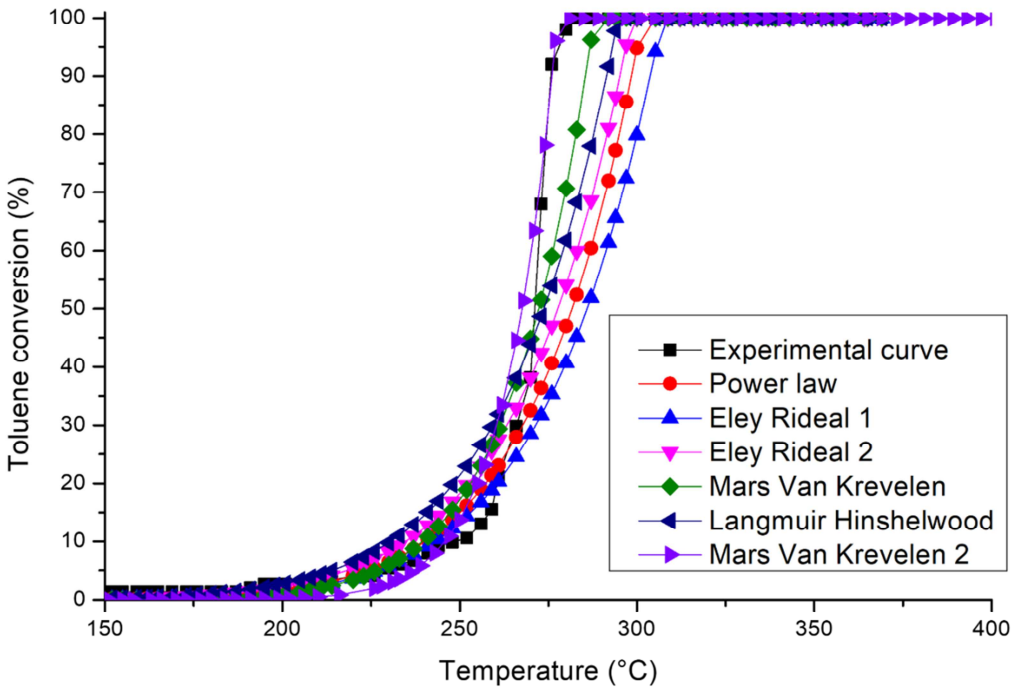

Figure 10: Comparison of the different models with the experimental curve

A well accordance is revealed for this model compared to the experimental model. Moreover, another MVK model has been tested. In this derived model, the chemical reaction taken into account is the oxidation of toluene to benzylic alcohol. This chemical equation is the first step for the total oxidation of toluene [53] in our case. A better accordance is obtained in this case. Thus, the Mars Van Krevelen modified mechanism described the total oxidation of toluene in presence of CoAlCe mixed oxide. The rate-determining step for this reaction in presence of CoAlCe mixed oxide corresponds to the oxidation of toluene to form the benzylic alcohol, following this model. Moreover, the description of the reaction by a Mars Van Krevelen mechanism permits to obtain values in accordance with the experimental data.

.Conclusion

In this study, the toluene total oxidation on CoAlCe mixed oxide has been modelled by eight models. In our case, the Mars Van Krevelen mechanism shows better accordance for modelling of this reaction. Moreover, the mechanism is *in adequation* with the experimental observation concerning the reduction of the Co_3O_4 species into CoO during the catalytic test with low concentration of oxygen. This observation indicates that the redox model is the most accurate model.

Acknowledgements

The authors thank the Industrial Environmental Research Institute (IRENI) and the European Community (Interreg IV France-Wallonie-Flandres project, REDUGAZ) for financial support.

References

[1] S. Ojala, N. Koivikko, T. Laitinen, A. Mouammine, P. Seelam, S. Laassiri, K. Ainassaari, R. Brahmi, R. Keiski, Catalysts 5 (2015) 1092–1151.

[2] S. Scirè, L.F. Liotta, Appl. Catal. B Environ. 125 (2012) 222–246.

[3] S. Ivanova, C. Petit, V. Pitchon, Gold Bull. 39 (2006) 3–8.

[4] E. Genty, L. Jacobs, T. Visart De Bocarmé, C. Barroo, Catalysts 134 (2017) 1–44.

[5] N.W. Cant, D.E. Angove, D.C. Chambers, Appl. Catal. B Environ. 17 (1998) 63–73.

[6] M.J. Patterson, D.E. Angove, N.W. Cant, Appl. Catal. B Environ. 26 (2000) 47–57.

[7] G. Centi, J. Mol. Catal. A Chem. 173 (2001) 287–312.

[8] T. Ataloglou, J. Vakros, K. Bourikas, C. Fountzoula, C. Kordulis, A. Lycourghiotis, Appl. Catal. B Environ. 57 (2005) 299–312.

[9] M. Baldi, V.S. Escribano, J.M.G. Amores, F. Milella, G. Busca, Appl. Catal. B Environ. 17 (1998) L175–L182.

[10] S.C. Kim, W.G. Shim, Appl. Catal. B Environ. 98 (2010) 180–185.

[11] A. Trovarelli, Catalysis by Ceria and Related Materials, Imperial C, World Scientific Publishing Company, 2002.

[12] W. Gao, Y. Zhao, J. Liu, Q. Huang, S. He, C. Li, J. Zhao, M. Wei, Catal. Sci. Technol. 3 (2013) 1324.

[13] L.F. Liotta, M. Ousmane, G. Di Carlo, G. Pantaleo, G. Deganello, A. Boreave, A. Giroir-Fendler, Catal. Letters 127 (2008) 270–276.

[14] K. Jiratova, P. Cuba, F. Kovanda, L. Hilaire, V. Pitchon, Catal. Today 76 (2002) 43–53.

[15] E. Genty, R. Cousin, S. Capelle, C. Gennequin, S. Siffert, Eur. J. Inorg. Chem. 2012 (2012) 2802–2811.

[16] C. Gennequin, S. Siffert, R. Cousin, A. Aboukaïs, Top. Catal. 52 (2009) 482–491.

[17] C.-W. Tang, M.-C. Kuo, C.-J. Lin, C.-B. Wang, S.-H. Chien, Catal. Today 131 (2008) 520–525.

[18] D.P. Debecker, E.M. Gaigneaux, G. Busca, Chemistry 15 (2009) 3920–35.

[19] C.-T. Chang, B.-J. Liaw, C.-T. Huang, Y.-Z. Chen, Appl. Catal. A Gen. 332 (2007) 216–224.

[20] L. a Palacio, J. Velásquez, A. Echavarría, A. Faro, F.R. Ribeiro, M.F. Ribeiro, J. Hazard. Mater. 177 (2010) 407–13.

[21] L.A. Palacio, J.M. Silva, F.R. Ribeiro, M.F. Ribeiro, Catal. Today 133–135 (2008) 502–508.

[22] S. Tanasoi, G. Mitran, N. Tanchoux, T. Cacciaguerra, F. Fajula, I. Săndulescu, D. Tichit, I.-C. Marcu, Appl. Catal. A Gen. 395 (2011) 78–86.

[23] J. Carpentier, S. Siffert, J.F. Lamonier, H. Laversin, a. Aboukaïs, J. Porous Mater. 14 (2006) 103–110.

[24] J. Carpentier, J.F. Lamonier, S. Siffert, E.A. Zhilinskaya, A. Abouka, Appl. Catal. A Gen. 234 (2002) 91–101.

[25] L.F. Liotta, H. Wu, G. Pantaleo, A.M. Venezia, Catal. Sci. Technol. 3 (2013) 3085.

[26] K. Jirátová, J. Mikulová, J. Klempa, T. Grygar, Z. Bastl, F. Kovanda, Appl. Catal. A Gen. 361 (2009) 106–116.

[27] M. Gabrovska, R. Edreva-Kardjieva, K. Tenchev, P. Tzvetkov, A. Spojakina, L. Petrov, Appl. Catal. A Gen. 399 (2011) 242–251.

[28] J. Pérez-Ramirez, G. Mul, J.A. Moulijn, Vib. Spectrosc. 27 (2001) 75–88.

[29] L.F. Liotta, G. Di Carlo, G. Pantaleo, A.M. Venezia, G. Deganello, Appl. Catal. B Environ. 66 (2006) 217–227.

[30] E. Genty, J. Brunet, C. Poupin, S. Casale, S. Capelle, P. Massiani, S. Siffert, R. Cousin, Catalysts 5 (2015) 851–867.

[31] E. Genty, J. Brunet, R. Pequeux, S. Capelle, S. Siffert, R. Cousin, Mater. Today Proc. 3 (2016) 277–281.

[32] J. Brunet, E. Genty, C. Barroo, F. Cazier, C. Poupin, S. Siffert, D. Thomas, G. De Weireld, T. Visart de Bocarmé, R. Cousin, Catalysts 8 (2018) 64.

[33] L. Matějová, P. Topka, K. Jirátová, O. Šolcová, Appl. Catal. A Gen. 443–444 (2012) 40–49.

[34] M. Hosseini, T. Barakat, R. Cousin, A. Aboukaïs, B.-L. Su, G. De Weireld, S. Siffert, Appl. Catal. B Environ. 111 (2012) 218–224.

[35] S. Velu, K. Suzuki, M.P. Kapoor, S. Tomura, F. Ohashi, T. Osaki, Chem. Mater. 12 (2000) 719–730.

[36] E. Genty, R. Cousin, S. Capelle, C. Gennequin, S. Siffert, Eur. J. Inorg. Chem. 2012 (2012) 2802–2811.

[37] V.R. Choudhary, G.M. Deshmukh, D.P. Mishra, Energy & Fuels 19 (2005) 54–

63.

[38] B. Miranda, E. Díaz, S. Ordóñez, A. Vega, F. V Díez, Chemosphere 66 (2007) 1706–15.

[39] C.I. Meyer, a Borgna, a Monzón, T.F. Garetto, J. Hazard. Mater. 190 (2011) 903–8.

[40] S. Krishnamoorthy, J.P. Baker, M.D. Amiridis, Catal. Today 40 (1998) 39–46.

[41] D. Delimaris, T. Ioannides, Appl. Catal. B Environ. 84 (2008) 303–312.

[42] K. Everaert, J. Baeyens, J. Hazard. Mater. 109 (2004) 113–39.

[43] G. Arzamendi, V. Delapenaoshea, M. Alvarezgalvan, J. Fierro, P. Arias, L. Gandia, J. Catal. 261 (2009) 50–59.

[44] J. Bedia, J.M. Rosas, J. Rodrigez-Mirasol, T. Cordero, Appl. Catal. B Environ. 94 (2010) 8–18.

[45] G. Saracco, F. Geobaldo, G. Baldi, A 20 (1999) 277–288.

[46] G. Arzamendi, V.A. de la Peña O'Shea, M.C. Álvarez-Galván, J.L.G. Fierro, P.L. Arias, L.M. Gandía, J. Catal. 261 (2009) 50–59.

[47] P. Mars, D.W. van Krevelen, Chem. Eng. Sci. 3 (1954) 41–59.

[48] S. Swislocki, K. Stöwe, W.F. Maier, J. Catal. 316 (2014) 219–230.

[49] E. McCullagh, J.B. McMonagle, B.K. Hodnett, Appl. Catal. A, Gen. 93 (1993) 203–217.

[50] S. Ordóñez, L. Bello, H. Sastre, R. Rosal, V.D. Fernando, Appl. Catal. B, Environ. 38 (2002) 139–149.

[51] B. Grbic, N. Radic, A. Terlecki-Baricevic, Appl. Catal. B Environ. 50 (2004) 161–166.

[52] C. He, P. Li, J. Cheng, Z.-P. Hao, Z.-P. Xu, Water, Air, Soil Pollut. 209 (2009) 365–376.

[53] E. Genty, PhD thesis, Université du Littoral Côte d'Opale, 2014.

Table 3: Summary of the kinetics values from the several model tested

Model	Characteristic	Reaction rate equation	Rate parameters [a]	Regression for : $x_{cal}=a.x_{exp}$ [b]	
				a	R^2
Power Law		$r = k\ {P_{tol}}^{n}{P_{O_2}}^{m}$	$k = 3.13\ 10^{10}\exp\left(\frac{-79.66\ 10^3}{RT}\right)$ n =-0.86 m = 0.10	1.0212	0.9498
Eley-Rideal 1 (ER1)	Toluene adsorbed O_2 in gaseous phase	$r = \frac{k_r\ K_{tol}P_{tol}P_{O_2}}{1 + K_{tol}P_{tol}}$	$k_r = 479.18\exp\left(\frac{-35.14\ 10^3}{RT}\right)$ $K_{tol} = 5.26\exp\left(\frac{15.06\ 10^3}{RT}\right)$	1.0347	0.9283
Eley-Rideal 2 (ER2)	O_2 dissociative adsorption Toluene in gaseous phase	$r = \frac{k_r\ P_{tol}\sqrt{K_{O_2}P_{O_2}}}{1 + \sqrt{K_{O_2}P_{O_2}}}$	$k_r = 1.5\ 10^5\exp\left(\frac{-62.21\ 10^3}{RT}\right)$ $k = 1.5\ 10^{-3}\exp\left(\frac{18.99\ 10^3}{RT}\right)$	0.987	0.9727
Langmuir Hinshelwood (L-H)		$r = \frac{KrK_{O_2}K_{tol}P_{tol}P_{O_2}}{(1 + K_{O_2}\ P_{O_2} + K_{tol}P_{tol})^2}$	$Kr = 9.92\ 10^{13}\exp\left(\frac{-85.510^3}{RT}\right)$ $K_{O_2} = 8.95\ 10^{-8}\exp\left(\frac{44.99\ 10^3}{RT}\right)$ $K_{tol} = 1253\exp\left(\frac{39.03\ 10^3}{RT}\right)$	0.9598	0.975
Mars Van Krevelen		$r = \frac{K_{O_2}\ K_{tol}P_{tol}P_{O_2}}{K_{O_2}\ P_{O_2} + 9K_{tol}P_{tol}}$	$K_{O_2} = 1.85\ 10^{10}\exp\left(\frac{-99.22\ 10^3}{RT}\right)$ $K_{tol} = 8.85\ 10^{11}\exp\left(\frac{-129.18\ 10^3}{RT}\right)$	1.0077	0.9818
Mars Van Krevelen 2	Reaction Toluene to benzylic alcohol	$r = \frac{K_{O_2}\ K_{tol}P_{tol}P_{O_2}}{K_{O_2}\ P_{O_2} + 0.5\ K_{tol}P_{tol}}$	$K_{O_2} = 2.313\ 10^{10}\exp\left(\frac{-92.01\ 10^3}{RT}\right)$ $K_{tol} = 7.02\ 10^{11}\exp\left(\frac{-120.26\ 10^3}{RT}\right)$	0.9981	0.9944

For the Power law model: k in $mol.Pa^{0.76}.h^{-1}.g^{-1}$, for the E-R models: kr in $mol.Pa^{-1}.h^{-1}.g^{-1}$, K_{tol} and K_{O2} in Pa^{-1}, for L-H model: $mol.g^{-1}.s^{-1}$; for MVK models : K_{tol} and K_{O2} in $mol.Pa^{-1}.h^{-1}.g^{-1}$

b Calculated (x_{cal}) versus experimental (x_{exp}) conversion; a: slope of regression line, R^2: sum of the squares

Toluene total oxidation
CoAlCe mixed oxide